Biochimica et Biophysica Acta 859 (1986) 257–265
Elsevier

BBA 73142

The kinetics of formation and structure of the low-temperature phase of 1-stearoyl-lysophosphatidylcholine

Jairajh Mattai and G. Graham Shipley

Biophysics Institute, Departments of Medicine and Biochemistry, Boston University School of Medicine, 80 East Concord Street, Boston, MA 02118 (U.S.A.)

(Received March 6th, 1986)

Key words: Kinetics; Low-temperature phase; Phase transition; 1-Stearoyl-lysophosphatidylcholine; X-ray diffraction; Differential scanning calorimetry

A combination of differential scanning calorimetry (DSC) and X-ray diffraction have been used to study the kinetics of formation and the structure of the low-temperature phase of 1-stearoyl-lysophosphatidylcholine (18:0-lysoPC). For water contents greater than 40 weight %, DSC shows a sharp endothermic transition at 27°C ($\Delta H = 6.75$ kcal/mol) corresponding to a low-temperature phase → micelle transition. This sharp transition is not reversible, but is regenerated in a time and temperature-dependent manner. For example, with incubation at 0°C the maximum transition enthalpy ($\Delta H = 6.75$ kcal/mol) is generated in about 45 min after an initial slow nucleation process of approx. 20 min. The kinetics of formation of the low-temperature phase is accelerated at lower temperatures and may be related to the disruption of 18:0-lysoPC micelles by ice crystal formation. X-ray diffraction patterns of 18:0-lysoPC recorded at 10°C over the hydration range 20–80% are characteristic of a lamellar gel phase with tilted hydrocarbon chains with the bilayer repeat distance increasing from 47.6 Å at 20% hydration to a maximum of 59.4 Å at 39% hydration. At this maximum hydration, approx. 19 molecules of water are bound per molecule of 18:0-lysoPC. Electron density profiles show a phosphate-phosphate distance of 30 Å, indicating an interdigitated lamellar gel phase for 18:0-lysoPC at all hydration values. The angle of chain tilt is calculated to be between 20 and 30°. For water contents greater than 40%, this interdigitated lamellar phase converts to the micellar phase at 27°C in a kinetically fast process, while the reverse (micelle → interdigitated bilayer) transition is a kinetically slower process (see also Wu, W. and Huang, C. (1983) Biochemistry 22, 5068–5073).

Introduction

Lysophospholipids, occurring in small quantities, are important components of biological membranes; among their functions are: (i) to act as lytic agents [1,2], (ii) to induce cell fusion [3], (iii) as an intermediate in phospholipid metabolism occurring in membranes during phospholipid turnover [4]. Their aqueous dispersions are also of interest since the physical properties of these dispersions are related to their biological function. Reiss-Husson [5] investigated egg lysophosphatidylcholine dispersions in water by X-ray diffraction, and the phase diagram was shown to consist of three regions: a micellar phase at high water content, a hexagonal Type I phase of cylindrical micelles at lower water content and a 'crystalline' phase at low temperatures. X-ray diffraction studies [6] showed that the low-temperature phase was lamellar. Recent studies by Eriksson et al. [7] on hydrated 1-palmitoyl-lysophosphatidylcholine have shown the existence of an additional cubic liquid crystalline phase (I_1), occurring in the phase diagram at water contents intermediate between that required to form the hexagonal and micellar phases.

The lamellar to micellar transition of lysoPC assemblies has been the focus of some recent investigations [8–10]. Structurally, this transition involves a reorganization from a planar bilayer arrangement to a highly curved micellar surface. The relatively large polar group of the lysoPC molecule relative to its hydrophobic chains gives it a 'wedge' or 'cone' shaped appearance. This shape allows the molecules to pack into micellar or cylindrical geometries, since these structural arrangements allow for optimal packing and shielding of the hydrophobic chains from water.

Because of the absence of a fatty acyl chain in the *sn*-2 position of lysoPC molecules, they are predicted to form interdigitated lamellar phases at low temperatures. ^{31}P-NMR studies of 1-palmitoyl-lysophosphatidylcholine by Van Echteld et al. [8] have demonstrated the existence of bilayers at low temperature and it was suggested that the acyl chains are interdigitated. X-ray diffraction of hydrated *n*-octadecylphosphocholine, a structural analogue of 18 : 0-lysoPC, at low temperatures also showed the existence of interdigitated bilayers [11].

Both the lamellar to micellar and micellar to lamellar transition of 18 : 0-lysoPC have recently been examined by a combination of diphenylhexatriene fluorescence anisotropy, ^{31}P-NMR, Raman spectroscopy, and high sensitivity differential scanning calorimetry [9,10]. While the lamellar to micellar transition is a rapid process, the reverse micellar to lamellar conversion occurs slowly with a negative temperature dependence. Further, the extended multilamellar structures at low temperatures show strong interchain interactions suggesting an interdigitated lamellar structure.

In the present investigation, differential scanning calorimetry (DSC) and X-ray diffraction have been used to examine the structure of the low temperature phase of 18 : 0-lysoPC over a range of hydration conditions. While data from ^{31}P-NMR and Raman spectroscopy [9] suggest the presence of an interdigitated gel phase for this lysoPC, no direct structural data is available to support this conclusion. Rand et al. [6] have interpreted their X-ray diffraction data from egg lysophosphatidylcholine (containing 80% 1-palmitoyl-lysoPC and 20% 18 : 0-lysoPC) in terms of hydrocarbon chain tilting. No structural data is available for hydration studies of 18 : 0-lysoPC. In this study, 18 : 0-lysoPC is examined over the hydration range (20–90 weight %), using DSC to define the kinetics of the micellar → lamellar transition observed at high water content, and using X-ray diffraction to define the structure of the low temperature lamellar phase at all hydration levels.

Materials and Methods

18 : 0-lysoPC was obtained from Avanti Polar Lipids, Inc. (Birmingham, AL) and was judged to be pure by the appearance of a single spot on TLC plates using the solvent system $CHCl_3/CH_3OH/NH_3/H_2O$ (25 : 17 : 2.5 : 2.5, v/v).

Sample preparation. For DSC, samples of anhydrous 18 : 0-lysoPC were weighed directly into stainless steel pans and appropriate amounts of distilled, deionized water were added gravimetrically corresponding to the hydration range 10–90 weight %.

Hydrated samples for X-ray diffraction were prepared by weighing anhydrous 18 : 0-lysoPC directly into thin-walled quartz capillary tubes (internal diameter 1 mm) followed by gravimetric addition of distilled, deionized water. Samples were covered with parafilm, centrifuged at room temperature for about 2 min, then flame-sealed. For the hydration range 40–90%, the dispersions were homogenized through the cycle centrifugation-sample inversion-centrifugation at a temperature above the transition temperature. Below 40% hydration, the flame-sealed samples were homogenized by centrifugation at approx. 15 000 rpm in a high-speed Sorval centrifuge (DuPont Co., Wilmington, DL).

Methods. Calorimetric measurements were performed with a Perkin-Elmer (Norwalk, CT) DSC-2 differential scanning calorimeter. Samples were heated above the phase transition temperature and cooled, and the cycle repeated at least three more times at a heating/cooling rate of 5 K/min. The samples were then stored at −4°C for several days. For kinetic studies, the equilibrated samples were heated above the transition temperature, cooled at 5 K/min and held at 0°C for various periods of time followed by a heating and cooling cycle. Samples were also cooled to −28°C, below the temperature of the water-ice transition, followed by immediate reheating. The maxima in the

heat capacity versus temperature plots were taken as the phase transition temperatures while the transition enthalpies were determined from the area under the curve as measured by planimetry, and compared with the known enthalpy of a Ga standard.

X-ray diffraction patterns were recorded with photographic films using nickel-filtered CuK_α X-radiation from an Elliot GX-6 rotating anode generator (Elliot Automation, Borehamwood, U.K.), which was collimated by double mirror optics or toroidal optics into a point source. Microdensitometry of X-ray diffraction photographs was carried out using a Joyce Loebl model III-CS microdensitometer.

Results

Differential scanning calorimetry

Representative DSC heating curves of 18 : 0-lysoPC over the hydration range 10–70 weight% are shown in Fig. 1a. These endotherms were obtained following incubation of the samples at −4°C for several days or after cooling the samples down through the ice transition to −28°C followed by immediate reheating. On cooling to −4°C, single relatively sharp exothermic transitions are observed at low hydrations (10–20%). An increase in transition width and the presence of multiple transitions are observed at intermediate hydration levels (20–50%). However, at high water contents (> 70%) no exothermic transition is observable on cooling (see Fig. 2b). At intermediate and high water content, immediate reheating produced endotherms which were not reproducible in terms of either transition temperature (T_m) or enthalpy; the enthalpy was always smaller on immediate reheating (see Fig. 2c).

At 10% hydration, the 18 : 0-lysoPC shows a low-enthalpy transition at approx. 8.5°C (ΔH = 0.14 kcal/mol) together with a sharp cooperative transition at 62.2°C (ΔH = 6.8 kcal/mol). On increasing the hydration to 20%, the low temperature transition is not observed and the high-temperature transition becomes broader and less cooperative with a peak width at half-height of 7.5 K (T_m = 51.4°C, ΔH = 6.4 kcal/mol). Further hydration to 30% leads to increased broadening of the endothermic transition with a peak width at half-height of 9.3 K and a reduced transition temperature of 43°C (ΔH = 6.4 kcal/mol). With increasing water content the transition endotherm sharpens and for water contents above 50%, the transition temperature is constant at 27°C. The transition temperature versus weight % water curve (Fig. 1b), shows the decrease in transition temperature from 62.2°C at 10% hydration to 27°C between 40 and 50% hydration, with no further change of T_m with increasing hydration. The transition enthalpy data (Fig. 1c) show an almost constant enthalpy value of 6.7 kcal/mol over the hydration range 10–90%. This constant transition enthalpy observed over a large hydration range for 18 : 0-lysoPC differs from that observed in other phospholipid systems where ΔH is found to increase to a maximum at maximum hydration.

As mentioned previously, the DSC heating curves shown in Fig. 1a were obtained by incubating the samples at −4°C over a period of time (several days) followed by immediate reheating. From the cooling and reheating curves it is clear that the low temperature phase of 18 : 0-lysoPC is generated in a time- and temperature-dependent manner. In the next section we describe the kinetics of formation of the low-temperature lamellar phase for a completely hydrated sample where the micellar phase exists above T_m.

Kinetics of the micellar → lamellar transition of 90% hydrated 18 : 0-lysoPC at 0°C

In Fig. 2a, the DSC heating curve of a 90% hydrated sample of 18 : 0-lysoPC after incubation for several days at −4°C is shown. A single sharp transition at 27.0°C is observed with an enthalpy of 6.75 kcal/mol. On cooling to 0°C no exothermic transition is observed (Fig. 2b), and immediate reheating also shows no endothermic transition (Fig. 2c). The lamellar → micellar transition of 18 : 0-lysoPC is clearly not reversible. In Fig. 2c–k, DSC heating curves for the excess hydrated sample of 18 : 0-lysoPC, incubated for various periods of time at 0°C, are presented. During the initial stages of incubation between 0 and 20 min (Fig. 2c–f), little enthalpy is generated. Thereafter, the transition enthalpy increases rapidly (Fig. 2g–j) until the conversion to the low temperature phase is completed in approx. 45 min. The enthalpy of the 27°C transition is plotted as a

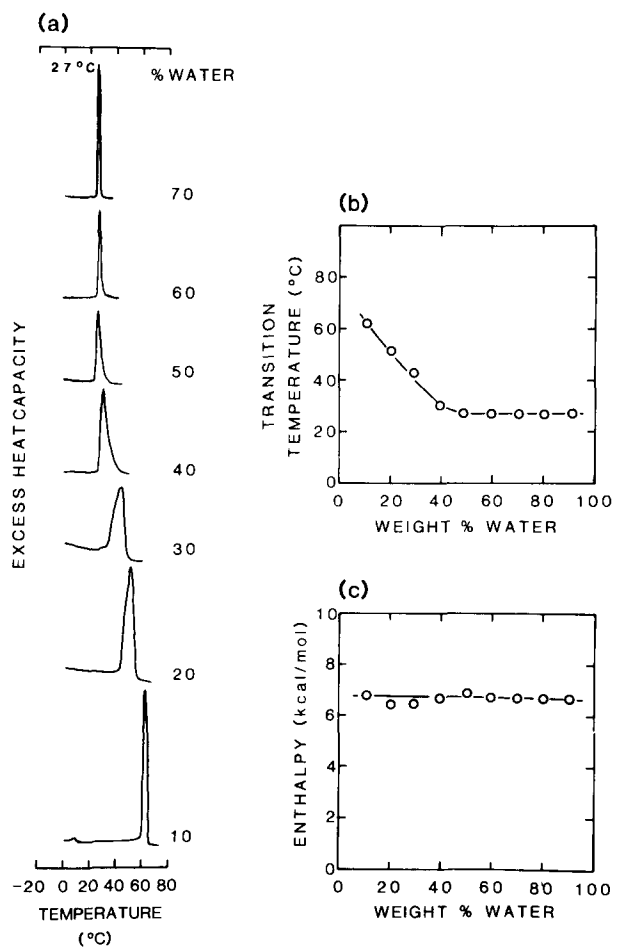

Fig. 1. (a) DSC heating curves (heating rate 5 K/min) of 18:0-lysoPC after incubation at −4°C at different degrees of hydration; (b) transition temperature (T_m) and (c) transition enthalpy as a function of water content determined from endotherms in (a).

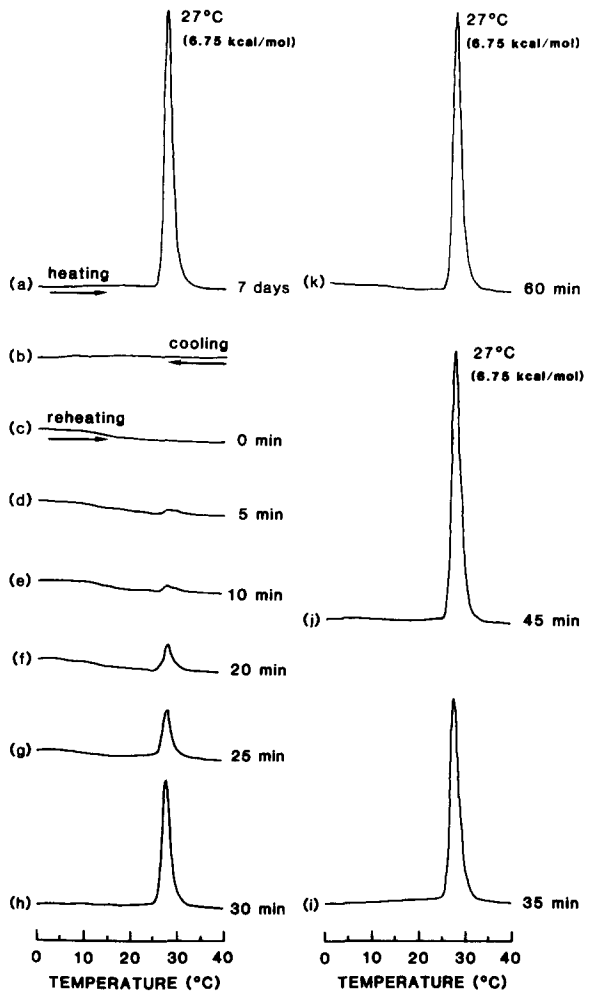

Fig. 2. DSC heating curves which illustrate the kinetics of the lamellar ↔ micellar transition of 18:0-lysoPC (90% hydrated). (a) Heating curve after incubation for 7 days at −4°C; (b) corresponding cooling curve; (c)–(k) heating curves after incubation for different periods of time at 0°C.

function of incubation time at 0°C in Fig. 3. Within the first 20 min, the transition enthalpy increases slowly to approx. 0.6 kcal/mol, with the peak maximum at approx. 27.7°C. By 30 min, the enthalpy has increased considerably to approx. 3.0 kcal/mol with a sharpening of the transition and by 45 min the enthalpy has more than doubled to its maximum value of 6.75 kcal/mol and T_m = 27.0°C. There is evidently an initial lag time of about 20–25 min during which a slow nucleation process occurs, followed by a rapid cooperative low-temperature phase formation over the next 15–20 min generating the maximum enthalpy, which does not change on further incubation. Also included in Fig. 3 is the enthalpy data for the excess hydrated sample cooled below the ice transition to −28°C followed by immediate reheating. The enthalpy is identical to that generated after approx. 45 min incubation at 0°C. In the next section, we have examined the structure of the

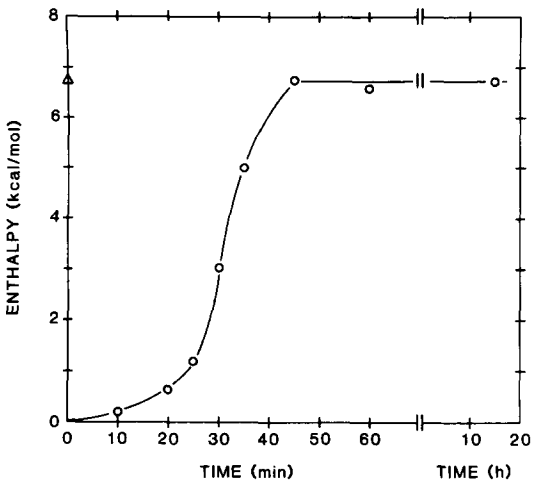

Fig. 3. (a) Transition enthalpy (from Fig. 2) versus incubation time at 0°C showing the formation of the lamellar phase from the micellar phase of 18:0-lysoPC (90% hydrated) (○); (b) transition enthalpy obtained after cooling the sample down through the water → ice transition to −28°C followed by immediate reheating (△).

low-temperature phase of 18:0-lysoPC at 10°C over a range of hydration conditions using X-ray diffraction.

X-ray diffraction of hydrated 18:0-lysoPC at 10°C

X-ray diffraction patterns of 18:0-lysoPC have been obtained over the hydration range (20–80%) at 10°C i.e., at a temperature well below the phase transition temperature, T_m. Diffraction patterns of samples below 20% hydration were not recorded because of difficulties in producing homogeneous samples. A representative X-ray diffraction pattern of a 20% hydrated sample of 18:0-lysoPC at 10°C is shown in Fig. 4a. Several low angle reflections were observed indexing in the ratio $1:1/2:1/3:1/4\ldots$, characteristic of a one-dimensional lamellar lattice. At higher scattering angles, a sharp reflection at 4.3 Å together with a broader reflection at 4.1 Å are observed. This type of diffraction pattern is characteristic of gel phase bilayers with tilted hydrocarbon chains and hexagonal chain packing, analagous to the $L_{\beta'}$ phase of dimyristoylphosphatidylcholine (DMPC) and dipalmitoylphosphatidylcholine (DPPC) [12–14]. With increasing water content up to 40% (Fig. 4b), the low-angle region shows lamellar reflections with changes occurring in both the position and

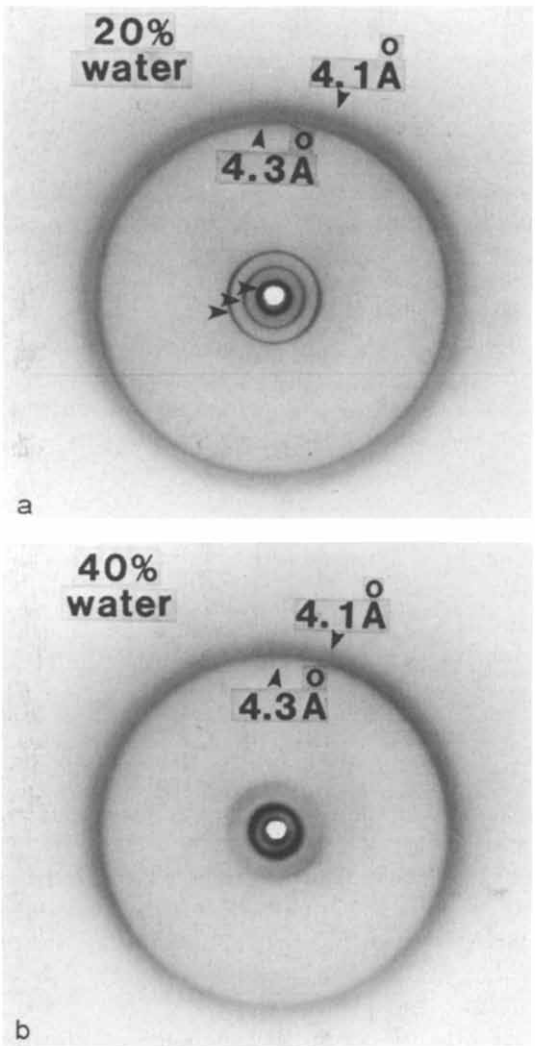

Fig. 4. X-ray diffraction patterns of (a) 20% hydrated and (b) 40% hydrated 18:0-lysoPC at 10°C. Arrows indicate the low-angle lamellar reflections and wide-angle reflections noted in text.

intensity of the reflections. The two wide-angle reflections do not change significantly over this hydration range (c.f., Figs. 4a and 4b).

In order to determine the structural features of this one-dimensional lattice we have analyzed the low-angle X-ray diffraction data at different degrees of hydration. In Fig. 5, the hydration dependence of the lamellar repeat (d) is shown together with the calculated structural parameters, lipid thickness (d_l), water thickness (d_w) and surface

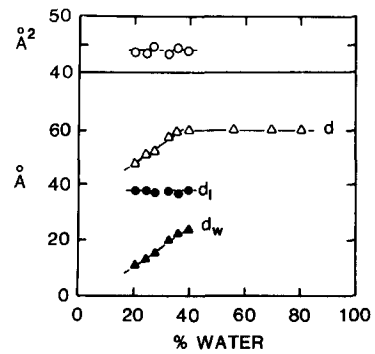

Fig. 5. Variation of the structural parameters of 18:0-lysoPC as a function of water content at 10°C. △: bilayer repeat, d; ●: lipid thickness, d_l; ▲: thickness of the water layer, d_w; ○: area of one 18:0-lysoPC molecule at the lipid/water interface.

area per lipid molecule (S), determined from the lamellar repeat distance using the equations of Luzzati [15]. The unilamellar repeat distance increases from 47.6 Å at 20.6% water to a limiting value of 59.4 Å for water contents greater than 40%. These values are somewhat higher than that determined for egg lysophosphatidylcholine at 22°C by Rand et al. [6]. The calculated lipid thickness and surface area remain relatively constant at approx. 37 Å and approx. 44 Å^2 over the range 20–40% H_2O. In the absence of partial specific volume, $\bar{v}$, measurements of hydrated 18:0-lysoPC at 10°C, we have assumed a value of 0.93 cm^3/g similar to gel phase DPPC [16] to calculate d_l and S.

The intensities of the low-angle reflections were measured for different degrees of hydration (20–50%) and were found to vary with water content. For example, at 20.6% H_2O, the fourth-order reflection is not detectable, but increases in intensity with increasing hydration. While the third-order reflection at 20.6% H_2O content is quite strong, it decreases in intensity with increasing hydration. Providing that the 'bilayer' structure itself does not change significantly with hydration [17], the swelling method [18–20] may be used to derive the unsampled structure amplitude curve for the 18:0-lysoPC structure. The observed lamellar intensities for each hydration were corrected for Lorentz and polarization factors ($I_{00l} \cdot l^2$) and each set scaled and normalized with respect to other sets using the method of Worthington and Blaurock [21], i.e.

$$\frac{1}{d}\sum_{l=1}^{N}\left(I_{00l}\cdot l^2\right) = \text{constant}$$

The scaled, normalized structure amplitudes ($|\sqrt{I\cdot l^2}|$) were plotted as a function of reciprocal space coordinate s ($= 2 \sin\theta/\lambda$) and are shown in Fig. 6. Clearly all of the amplitudes lie on the same curve and the nodes are located at $s \approx 0.013$, 0.05 and 0.08 Å^{-1} (arrows in Fig. 6) and represent the points at which a phase change could occur. Since the lipid bilayer at this resolution is a centrosymmetric structure the phases can be either 0 or π and thus the phase assignment is $0,\pi,0$ or $\pi,0,\pi$. Electron density profiles calculated at all hydrations according to the two phase choices show that only with $\pi,0,\pi$ does the lipid hydrocarbon chain region have a lower electron density than that of water. The electron density profiles corresponding to this phase choice are shown in Fig. 7a. The two high-density maxima correspond to the location of the electron-rich phosphate moiety of the polar head group of 18:0-lysoPC and the peak to peak separation $d_{P\text{-}P}$ is observed to be constant at approx. 30 Å over the hydration range 20–40%. The region of lower density on the outer edges of each profile corresponds to the region of the water layer and this increases in thickness with increasing hydration (see also the behavior of d_w in Fig. 5). The central area at 0 Å shows a region of medium electron density, unlike

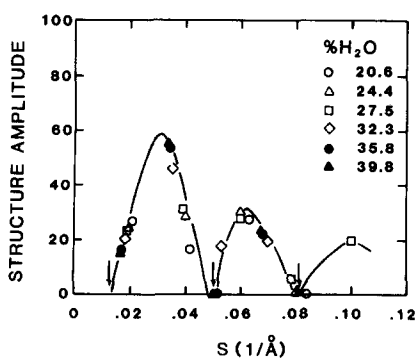

Fig. 6. Structure amplitudes versus reciprocal space coordinate, s ($= 2 \sin\theta/\lambda$), for 18:0-lysoPC at different degrees of hydration at 10°C. 2θ = diffraction angle; $\lambda = 1.5418$ Å. The solid line is drawn by eye.

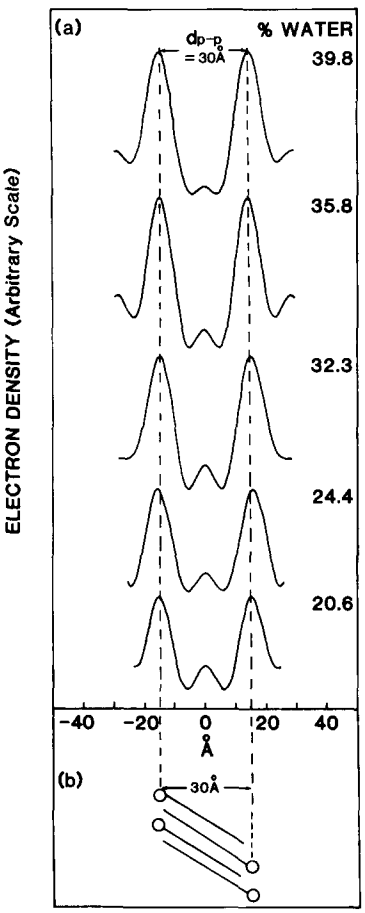

Fig. 7. (a) Electron density profiles for 18:0-lysoPC at 10°C over the hydration range 20–40%; (b) Model showing interdigitated, tilted chain bilayer.

that found in hydrated symmetric chain phosphatidylcholines [14] where a central trough of low electron density corresponding to the location of terminal methyls in the center of the bilayer is generally observed.

Discussion

The kinetics of the micellar → lamellar transition of fully hydrated 18 : 0-lysoPC show that after an initial slow nucleation process, the phase change is completed in about 45 min (see Fig. 3). These results are in good agreement with DSC measurements by Wu et al. [9] of dilute dispersions of 18 : 0-lysoPC in excess 50 mM KCl where the conversion to the low-temperature phase occurred in about 1 h. Wu et al. [9] have also shown that the micellar → lamellar transition has a negative temperature dependence, i.e. the low-temperature phase is generated at a faster rate at lower temperatures. Interestingly our data demonstrate that the formation of ice crystals at low temperatures induces an immediate conversion from the micellar phase to the low temperature phase. Presumably formation of ice crystals disrupts the micellar organization of 18 : 0-lysoPC allowing rapid conversion to the lamellar phase.

Our X-ray diffraction data for the low-temperature phase of 18 : 0-lysoPC at 10°C at all hydration levels show a lamellar gel phase. The wide angle diffraction data suggest that the hydrocarbon chains are tilted with respect to the bilayer normal and packed in a hexagonal array similar to that described for the $L_{\beta'}$ gel phase of various diacylphosphatidylcholines [12,14]. This gel phase swells to a maximum at approx. 39% hydration corresponding to approx. 19 molecules of water bound per molecule of 18 : 0-lysoPC. At maximum hydration, approx. 19 molecules of water were also calculated to be bound to the tilted $L_{\beta'}$ gel phase of 1,2-dipalmitoylphosphatidylcholine [22], which suggests that the amount of water bound is primarily a function of the phosphorylcholine polar group and independent of the hydrocarbon chains. The short phosphate-phosphate intrabilayer distance of 30 Å and the absence of a well defined central trough in the electron density profiles of Fig. 7a indicate that the hydrocarbon chains of 18 : 0-lysoPC are interdigitated. The shapes of the electron density profiles in Fig. 7a are quite similar to the electron density profiles of other interdigitated bilayer systems [23–26]. Note the approx. 7 Å difference between d_1, the calculated total bilayer thickness, and $d_{p\text{-}p}$, the separation of the phosphate groups, over the hydration range 20–40%; although a difference between these two measurements of lipid thickness is expected, errors in the assumptions implicit in the calculation of d_1, errors in the assumed valve of $\bar{v}$, and the low resolution of the profiles may exaggerate the difference. It should be emphasized that both methods show that the lipid thickness is insensitive to hydration changes, at least over the range 20–40% water. In both symmetric and asymmetric phosphatidylcholines [14,27] as well as

18 : 0-lysoPC, d_l is always found to be greater than $d_{p\text{-}p}$. Also included in Fig. 5 is the water thickness d_w which is shown to increase from 10.4 Å at 20% hydration to 22.3 Å at maximum hydration of approx. 39%.

Using the approach of Luzzati [15], we have calculated the average area available to one 18 : 0-lysoPC molecule at the lipid-water interface to be 44 Å^2. The area per hydrocarbon chain, determined from the wide-angle reflections (see Ref. 22), gave a value of 20.0 Å^2. Clearly there is sufficient area available to accomodate two hydrocarbon chains per head group, again consistent with chain interdigitation. However, the relative cross-sectional area of the head group (44 Å^2) has a larger excluded area in the plane of the bilayer than that occupied by two untilted gel state hydrocarbon chains (approx. 40 Å^2). In order for the chains to come into close contact and maximize van der Waals' interactions, they must tilt (see Fig. 7b) [28]. Direct evidence for chain tilting is indicated by the presence of two reflections at 4.3 Å and 4.1 Å in the wide-angle region of the X-ray diffraction pattern. In addition, we have calculated the angle of tilt of hydrated 18 : 0-lysoPC at 10°C using the crystal structure data of Hauser et al. [29] for tilted, interdigitated 1-lauroyl-propanediol-3-phosphorylcholine, an analogue of 18 : 0-lysoPC lacking the hydroxyl group in the *sn*-2 position of the glycerol backbone. If the hydrocarbon chains of 18 : 0-lysoPC are rigid and in an *all-trans* configuration, for an untilted interdigitated structure the phosphate-phosphate distance is calculated to be 33.5 Å and the total lipid thickness 40.0 Å, using the data of Hauser et al. [29]. Since the experimentally determined phosphate-phosphate distance is 30 Å (Fig. 7a) and the total lipid thickness is 37 Å (Fig. 5), then the angle of tilt is approx. 27° or 22° with respect to the normal to the plane of the bilayer using the two approaches. Allowing for errors and assumptions in the two calculations, an interdigitated structure with the chains tilted by 20–30° with respect to the bilayer normal is indicated.

A summary of the structure and behavior of fully hydrated 18 : 0-lysoPC is shown in Fig. 8. The transition from the interdigitated, tilted lamellar gel phase to the micellar phase is a rapid process. On cooling, the micellar phase slowly converts to the tilted interdigitated gel phase by way of an initial slow nucleation process followed by a rapid conversion, the complete phase change occurring in approx. 45 min at 0°C. At lower hydration levels liquid-crystalline phases (e.g., hexagonal I, cubic, etc.) are present above T_m. The kinetics of the interconversions between these phases and the low temperature, interdigitated gel phase are complex and merit further study.

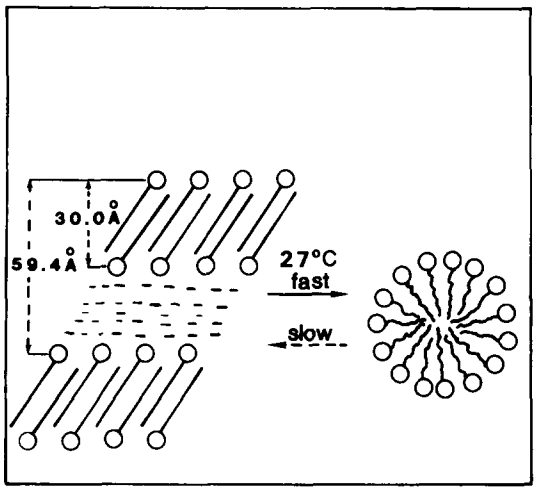

Fig. 8. Summary of the structural changes of fully hydrated 18 : 0-lysoPC during the lamellar ↔ micellar transtion.

Note added in proof: (Received June 19th, 1986)

Since the submission of this manuscript, an X-ray diffraction study focusing on the structure of the low temperature phase of 18 : 0-lysoPC has been published [30]. This study concludes similarly that the low temperature bilayer phase is interdigitated although these authors' data suggest that the chain tilt may be hydration and/or temperature dependent.

Acknowledgements

We wish to thank Mr. D. Jackson and Dr. D. Atkinson for assistance and useful discussions. We thank Irene Miller for help in preparing the manuscript. This research was supported by research grant HL-26335 and training grant HL-07291 from the National Institutes of Health.

References

1 Reman, F.C. and Van Deenen, L.L.M. (1967) Biochim. Biophys. Acta 137, 592–594
2 Reman, F.C., Demel, R.A., de Gier, J., Van Deenen, L.L.M., Eibl, H. and Westphal, O. (1969) Chem. Phys. Lipids 3, 221–223
3 Gledhill, B.L., Sawicki, W., Croce, C.M. and Koprowski, H. (1972) Exp. Cell Res. 73, 33–40
4 Ferber, E. (1973) in Biological Membranes (Chapman, D., and Wallach, D.F.H., eds.), pp. 221–252, Academic Press, London
5 Reiss-Husson, F. (1967) J. Mol. Biol. 25, 363–382
6 Rand, R.P., Pangborn, W.A., Purdon, A.D. and Tinker, D.O. (1975) Can. J. Biochem. 53, 189–195
7 Eriksson, P., Lindblom, G. and Arvidson, G. (1985) J. Phys. Chem. 89, 1050–1053
8 Van Echteld, C.J.A., De Kruijff, B., Mandersloot, J.G. and De Gier, J. (1981) Biochim. Biophys. Acta 649, 211–220
9 Wu, W., Huang, C., Conley, T.G., Martin, R.B. and Levin, I.W. (1982) Biochemistry 21, 5957–5961
10 Wu, W. and Huang, C. (1983) Biochemistry 22, 5068–5073
11 Jain, M.K., Crecely, R.W., Hille, J.D.R., De Haas, G.H. and Gruner, S.M. (1985) Biochim. Biophys. Acta 813, 68–76
12 Tardieu, A., Luzzati, V. and Reman, F.C. (1973) J. Mol. Biol. 75, 711–733
13 Janiak, M.J., Small, D.M. and Shipley, G.G. (1976) Biochemistry 15, 4575–4580
14 Janiak, M.J., Small, D.M. and Shipley, G.G. (1979) J. Biol. Chem. 254, 6068–6078
15 Luzzati, V. (1968) in Biological Membranes (Chapman, D., ed.), pp. 71–123, Academic Press, London and New York
16 Nagle, J.F. and Wilkinson, D.A. (1978) Biophys. J. 23, 159–175
17 Torbet, J. and Wilkins, M.H.F. (1976) J. Theor. Biol. 62, 447–458
18 Perutz, M.F. (1954) Proc. R. Soc. A. 225, 264–286
19 Moody, M.F. (1963) Science (Washington, D.C.) 142, 1173–1174
20 Worthington, C.R., King, G.I. and McIntosh, T.J. (1973) Biophys. J. 13, 480–494
21 Worthington, C.R. and Blaurock, A.E. (1969) Biophys. J. 9, 970–990
22 Ruocco, M.J. and Shipley, G.G. (1982) Biochim. Biophys. Acta 691, 309–320
23 Ranck, J.L., Keira, T. and Luzzati, V. (1977) Biochim. Biophys. Acta 488, 432–441
24 McIntosh, T.J., McDaniel, R.V. and Simon, S.A. (1983) Biochim. Biophys. Acta 731, 109–114
25 Serrallach, E.N., Dijkman, R., De Haas, G.H. and Shipley, G.G. (1983) J. Mol. Biol. 170, 155–174
26 Ruocco, M.J., Siminovitch, D.J. and Griffin, R.G. (1985) Biochemistry 24, 2406–2411
27 McIntosh, T.J., Simon, S.A., Ellington, J.C., Jr. and Porter, N.A. (1984) Biochemistry 23, 4038–4044
28 Hauser, H., Pascher, I., Pearson, R.H. and Sundell, S. (1981) Biochim. Biophys. Acta 650, 21–51
29 Hauser, H., Pascher, I. and Sundell, S. (1980) J. Mol. Biol. 137, 249–264
30 Hui, S.W. and Huang, C. (1986) Biochemistry 25, 1330–1335